

**PRESERVED FLORA AND ORGANICS IN IMPACT MELT BRECCIAS.** P. H. Schultz<sup>1</sup>, R. Scott Harris<sup>2</sup>, S. J. Clemett<sup>3</sup>, K. L. Thomas-Keptra<sup>3</sup> and M. Zárate<sup>4</sup>, <sup>1</sup>Department of Geological Sciences, Brown University, Providence, RI 02912 ([peter\\_schultz@brown.edu](mailto:peter_schultz@brown.edu)), <sup>2</sup>Office of Materials and Testing, GA Department of Transportation, Forest Park, GA 30297, <sup>3</sup>Jacobs, Houston, TX 77058, <sup>4</sup>CONICET/FCEN-Universidad Nacional de la Pampa, Santa Rosa, La Pampa, Argentina.

**Introduction:** At least seven glass-bearing strata of varying ages occur at different horizons in the Pampean sediments of Argentina dating back to the Miocene [1-4]. In a strict sense, these impact glasses are melt-matrix breccias composed of partially digested minerals clasts and basement fragments indicative of crater excavation. <sup>40</sup>Ar/<sup>39</sup>Ar dating yield ages ( $\pm 2\sigma$ ) of  $6 \pm 2$  Ka,  $114 \pm 26$  Ka,  $230 \pm 30$  Ka,  $445 \pm 21$  Ka,  $3.27 \pm 0.08$  Ma (near Mar del Plata = *MdP*),  $5.28 \pm 0.04$  Ma, and  $9.21 \pm 0.08$  Ma (near Chasico = *CH*) [4]. Where found in place (not reworked), these ages are consistent with the local stratigraphy and faunal assemblages [5]. A striking property of some of these impact glasses is the encapsulation of preserved fragments of floral [6,7] (and even soft-tissue faunal remains [7]). Here we identify retained organics and describe a likely process of encapsulation and preservation.

**Analyses:** Entrained centimeter-scale leaf fragments in some impact glasses exhibit remarkable preservation [7]. Parallel and striated assemblages containing vein-like features resemble vascular bundles found in tracheophytes such as pampas grass (Fig. 1A). Electron microprobe analyses of the surface of these materials closely match the composition of the impact glass, indicative of rapid quenching [7]. At higher magnifications, the striated assemblages become subparallel rows of phytoliths (Figs. 2A,B). Individual phytoliths range from  $\sim 7 - 12$  mm in diameter (Fig. 2A). Intermingled among the phytoliths is a disorganized fibrous matter (Fig. 2B), interpreted as degraded cellular material in various states of preservation (and blade-shaped phyllosilicate bundles (Fig. 2C). *EDX* (light element energy dispersive X-ray spectrometry) analyses of both the cellular material and associated phyllosilicates demonstrate the presence of major (*i.e.*,  $\geq 1$  wt. %) amounts of C (Figs. 2D,E).

*TEM* analyses of ultra-microtomed thin sections of *MdP* and *CH* samples reveal intermixed assemblages of four texturally and chemically distinct phases: (a) degraded plant matter, (b) impact glass, (c) phyllosilicate-rich bundles, and (d) mineral grains. The portions of degraded plant matter appear structure-less and selected area electron diffraction indicates it is amorphous. *EDX* point spectra revealed that the major elements present were C, O, Mg, Al, Si & Fe, with the C abundance enriched  $\sim 4\times$  over that of the surrounding glass. Bundles of phyllosilicates border

some of the glass and also occur embedded within the plant matter. Lattice spacing of  $\sim 1.0 - 1.1$  nm is consistent with smectite-type clays, with abundances (C, O, Mg, Al, Si & Fe) similar to expectations, albeit with excess Si and major C. Lattice spacings of  $\sim 1.0 - 1.1$  nm is consistent with smectite-type clays, with abundances (C, O, Mg, Al, Si & Fe) similar to expectations, albeit with excess Si and major C.

*Two-Step Laser Mass Spectrometry Analysis* ( $\mu$ -*L*<sup>2</sup>*MS*) revealed the presence and nature of organic materials. Analyses used both ultraviolet (UV) and vacuum ultraviolet (VUV) photo-ionization. UV-photo-ionization is selective to the presence of aromatic and/or conjugated organic species [8], whereas VUV-photo-ionization provides a broad window for most organic species [9].

Figure 3 summarizes the results from the analysis of several *MdP* samples. Figure 3A shows summed mass spectra acquired from embedded vascular material located  $\sim 100\mu\text{m}$  from the glass interface. The UV photo-ionization spectrum indicates a range of simple polycyclic aromatic hydrocarbons (PAHs) and their alkylated moieties; the most prominent being *C<sub>n</sub>-styrene* ( $\text{C}_6\text{H}_5\text{CH}=\text{C}(\text{CH}_2)_n\text{H}$ ;  $n = 0, 1 \rightarrow 104, 118$  amu), *C<sub>n</sub>-naphthalene* ( $\text{C}_{10}\text{H}_8-(\text{CH}_2)_n\text{H}$ ;  $n = 0, 1, 2 \rightarrow 128, 142, 156$  amu) and *C<sub>n</sub>-phenanthrene* ( $\text{C}_{14}\text{H}_{10}-(\text{CH}_2)_n\text{H}$ ;  $n = 0, 1, 2 \rightarrow 178, 192, 206$  amu). Additionally, there is evidence for oxidized substituents in the form of hydroxy (*-OH*) and methoxy (*CH<sub>3</sub>O-*) functional groups, *e.g.*, phenol ( $\text{C}_6\text{H}_5\text{OH}$ ; 94 amu). The VUV photoionization spectrum indicates that the overall abundance of organic matter is dominated by short chain (*C<sub>2</sub> - C<sub>6</sub>*) alkanes and alkenes.

Figure 3B shows summed mass spectra acquired from vascular material located farther ( $\sim 1000\mu\text{m}$ ) from the impact glass interface. The abundance of aromatic organics increases by over an order of magnitude, with a prominent cluster of higher mass peaks (*i.e.*,  $> 300$  amu) at 306, 312 and 318 amu.

Several inferences are possible: (a) the species are aromatic; (b) the preponderance of lower odd-mass peaks implies N-contain functionalities; (c) the main 312 amu peak has an exact mass of  $312.15 \pm 0.01$  amu, requiring  $\sim 20$  H atoms per molecule; and (d) the peaks intensities suggests a particularly stable species. Given the nature of the samples, tetracyclic pyrrole/pyrroline structures are consistent with these observations. For

example, the chlorin ( $C_{20}H_{16}N_4$ ; 312.14 amu) is the core macrocycle in chlorophyll and related photosensitive pigments in chloroplasts. Closely related to chlorin is chorin ( $C_{19}H_{22}N_4$ ; 312.14 amu), and corrinoid ring structures also occur naturally in biological systems.

**Entrapment Process:** A sequence of heating experiments constrained the conditions necessary for preserving plant matter within glass. In order to simulate a natural system, samples were prepared by adding small leaf clippings of Argentinean pampas grass, both wetted and un-wetted (but not desiccated), to pulverized *CH* impact glass. These were then flash-heated for 10, 60 & 300 seconds in a vertical-tube furnace at temperatures from 1,000 - 1,700°C. For each time and temperature three sample runs were performed at successively lower  $O_2$  fugacities by: (1) using an open Pt crucible; (2) using an open Pt crucible with a graphite rod; and, (3) using a sealed graphite tube and then quenched in ambient air.

We found that temperature is the critical variable. Below 1500°C the fused glass assemblages invariably contained carbonized leaf fragments, erasing both micro- and macro-scale leaf morphology. Above 1500°C, leaf morphology was preserved, and the visual appearance of the fused glass assemblages bore a striking resemblance to the natural samples. The survival of organic matter under these conditions requires: (a) the duration of the thermal excursion is short enough (*i.e.*, seconds) to prevent thermodynamic equilibrium; and, (b) the local peak temperature is buffered by energy sinks such as the endothermic phase transitions. The most likely process of entrainment is encapsulation during ejection from the transient crater or by near-rim ballistic melts landing in a swampy environment. Sediments such as loess appear to be a necessary condition for this process.

**Conclusions:** Flora matter embedded in Argentine *MdP* and *CH* impact glasses demonstrate that the cratering process and capture and preserve organic matter, thereby providing a strategy for identifying biomarkers of possible early life on Mars [10]. Broad areas on Mars are covered by loess and should have trapped impact melt over eons under conditions conducive for preservation until exhumed [11].

**References:** [1] Schultz, P.H. *et al.* (1994), *Geology* 22, 889-892; [2] Schultz, P.H. *et al.* (1998), *Science* 282, 2061-2063; [3] Schultz, P.H. *et al.* (2004), *EPSL* 219, 221-238; [4] Schultz, P.H. *et al.* (2006), *MAPS* 41, 749-771; [5] Zárate, M. (2003), *Quat. Sci. Revs.* 22, 1987-2006; [6] Schultz, P. H. and Harris, R. S. (2005), Abstracts of the Eighth NASA Exobiology PI Meeting; [7] Harris, R. S. and Schultz, P. H. (2007), *LPSC* 38, #2306; [8] Clemett, S.J., and Zare, R.N. (1996), in *IAU Symp.* 178: *Molecules in Astrophysics: Probes & Processes*, p. 305; [9] Shi, Y.J., and Lipson, R.H. (2005), *Canadian Journal of Chemistry* 83, 1891-1902; [10] Parnell, J. *et al.* (2007), In *Biological Processes Associated*

*with Impact Events*, ISSN: 1612- 8338; [11] Schultz, P.H., and Mustard, J. (2004), *J. Geophys. Res.* 109, E01001, doi: 10.1029/2002 JE002025.

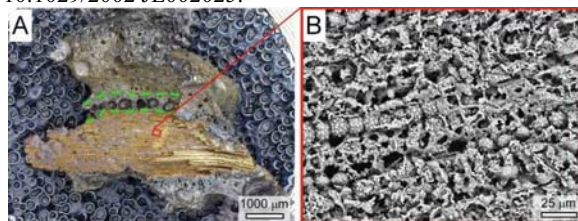


**Figure 1:** Optical (A) and SEM images (B) of a freshly exposed leaf preserved in *MdP* in impact glass. Dashed green lines indicate surrounding frothy rim. Backscatter SEM image of region (red box in A), showing cellular-scale preservation of structures including papillae and phytoliths.

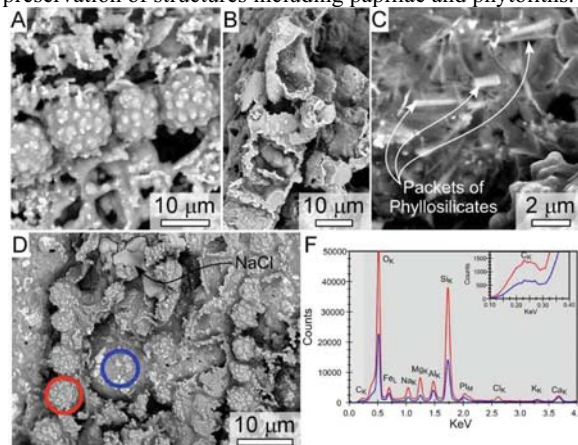


**Figure 2.** SEM images and EDX spectra of leaf fragment from Fig. 1. (A) Linear chain of phytoliths. (B) Edge on view of a sheet of cells; (C) Packets of phyllosilicates dispersed within leaf remnant; (D) SEM image; and (E) associated EDX spectra (red and blue circles) with the C enrichment associated with phytoliths and phyllosilicates packets.

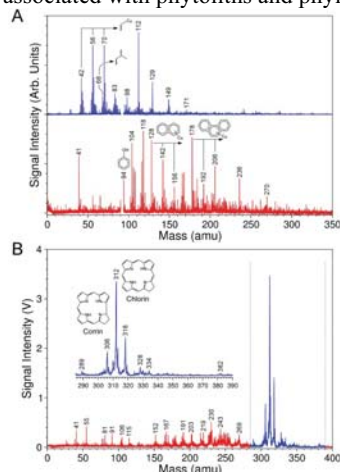


**Figure 3.** Mass spectra ( $\mu$ - $L^2$ MS) of preserved leaf fragment in *MdP* impact glasses. (A) Spectra using VUV (118 nm; blue) and UV (266 nm; red) photo-ionization of leaf material in close proximity ( $\sim 100 \mu\text{m}$ ) to the glass interface. (B) Spectra using UV photo-ionization located at distance ( $> 1000 \mu\text{m}$ ) from glass interface with enlarged section of VUV.